CHEMISTRY
A EUROPEAN JOURNAL

DOI: 10.1002/chem.200902963

# Reversible Dimerization of EGFR Revealed by Single-Molecule Fluorescence Imaging Using Quantum Dots

Nagako Kawashima,[a, b] Kenichi Nakayama,[a] Kohji Itoh,[b] Tamitake Itoh,[a] Mitsuru Ishikawa,[a] and Vasudevanpillai Biju*[a]

**Abstract:** The current work explores intermolecular interactions involved in the lateral propagation of cell-signaling by epidermal growth factor receptors (EGFRs). Activation of EGFRs by binding an EGF ligand in the extracellular domain of the EGFR and subsequent dimerization of the EGFR initiates cell-signaling. We investigated interactions between EGFRs in living cells by using single-molecule microscopy, Förster resonance energy transfer (FRET), and atomic force microscopy. By analyzing time-correlated intensity and propagation trajectories of quantum dot (QD)-labeled EGFR single molecules, we found that signaling dimers of EGFR [(EGF-EGFR)$_2$] are continuously formed in cell membrane through reversible association of heterodimers [EGF(EGFR)$_2$]. Also, we found that the lateral propagation of EGFR activation takes place through transient association of a heterodimer with predimers [(EGFR)$_2$]. We varified the transient association between activated EGFR and predimers using FRET from QD-labeled heterodimers to Cy5-labeled predimers and correlated topography and fluorescence imaging. Without extended single-molecule fluorescence imaging and by using bioconjugated QDs, reversible receptor dimerization in the lateral activation of EGFR remained obscured.

**Keywords:** biophysics · FRET · membrane proteins · quantum dots · signal transduction · single molecule studies

## Introduction

Intermolecular interactions of membrane proteins are often utilized by cells for regulating various biochemical and biophysical functions. A great variety of such functions are initiated by specific binding between ligands and receptors followed by conformational changes in the extracellular and cytoplasmic domains and clustering of receptor–ligand complexes.[1–10] For example, activation of epidermal growth factor receptor (EGFR) by binding an EGF ligand in EGFR and subsequent formation of EGFR dimers regulate cell signaling, growth, and proliferation.[6–15] However, the signal level in a cell is orders of magnitude higher than the number of signaling single molecules,[15] indicating that lateral propagation of EGFR activation cannot be underestimated in the amplification of cell-signaling and the regular growth and functioning of cells. Furthermore, enormous amplification of cell signaling by over-expressed EGFR results in the uncontrolled proliferation of many cancers.[16,17] Despite these significant relations between signaling by EGFR and life, the molecular mechanism underlying the lateral propagation of EGFR activation remains mostly unknown. Therefore, investigation of interactions among EGFR single molecules would unravel how an activated EGFR laterally activates a large number of predimers and may provide insight into the control of undesired cell-signaling related to various diseases.

Molecular forms of EGFR present in cells are predimers, heterodimers, and homodimers, or signaling dimers.[8–10] A heterodimer is formed when an EGF molecule activates one of the monomers in a predimer by binding in its extracellular domain, and a signaling dimer is formed when both the monomers are activated by two EGF molecules. However, signaling dimers are continuously formed, even without free

[a] N. Kawashima, Dr. K. Nakayama, Dr. T. Itoh, Dr. M. Ishikawa, Dr. V. Biju
Health Technology Research Center
National Institute of Advanced Industrial
Science and Technology (AIST)
2217-14 Hayashi-Cho, Takamatsu, Kagawa 761-0395 (Japan)
Fax: (+81) 878693558
E-mail: v.biju@aist.go.jp

[b] N. Kawashima, Dr. K. Itoh
Department of Medicinal Biotechnology
University of Tokushima, 1-78 Sho-Machi
Tokushima 770-8505 (Japan)

Supporting information for this article is available on the WWW under http://dx.doi.org/10.1002/chem.200902963.

EGF. This led to the suggestion that cooperative interactions among heterodimers and between predimers and heterodimers might be involved in the formation of signaling dimers.[11,15,18,19] Because of the significant properties of EGFR, the mechanism underlying its activation has been the subject of much investigation at both ensemble and single-molecule levels.[15,18–29] Due to the selectivity and sensitivity, single-molecule spectroscopy and microscopy have been widely exploited for addressing such intermolecular interactions as well as intramolecular conformational changes of molecules in solutions, on surfaces, at interfaces, and in cells.[30–44] For example, using single-molecule fluorescence imaging and Förster resonance energy transfer (FRET), Sako and co-workers have shown that EGFR activation through cooperative interactions between heterodimers and predimers is essential for cell-signaling.[15,18,24,25] Also, Bastiaens and co-workers have shown that restricted propagation of EGFR activation amplifies cell-signaling in human breast carcinoma cells.[19] More recently, Wiley and co-workers and others have shown that membrane cholesterol and the cytoskeleton restrict the propagation of EGFR signaling.[19,25,45–48] However, imaging and analyzing relatively slow and multiple events in the EGFR signaling pathway are considerably limited due to fast photobleaching of organic dyes.[15,18,24,25] For example, reversible dimerization of EGFR during the lateral propagation of activation remained obscured even in single-molecule experiments. Semiconductor quantum dots (QDs) on the other hand offer unique optical properties such as unusual photostability and bright photoluminescence for bioanalysis and bioimaging.[49–64] Thus, we employed QDs for investigating single-molecule EGFR activation.

In the current work, we combined the advantages of single-molecule imaging and unique optical properties of QDs and investigated multiple events in the lateral propagation of EGFR activation. We investigated EGFR activation by using single-molecule fluorescence imaging, FRET, and correlated AFM and optical microscopy imaging. EGFRs in living human ovarian epidermoid carcinoma cells (A431) were activated with QD-labeled human recombinant EGF. The activation was characterized by colocalizing Cy5-labeled mouse monoclonal EGFR antibody (Ab11) and QD-labeled EGF (Supporting Information). To make sure the colocalization occurred, we investigated FRET from QD-labeled EGF to Cy5-labeled Ab11. The molecular mechanism underlying the lateral propagation of EGFR activation was investigated by using fluorescence intensity trajectories and lateral propagation trajectories of single molecules, as well as FRET. We found that the lateral propagation of EGFR activation takes place through transient association of a heterodimer [EGF(EGFR)$_2$] with predimers [(EGFR)$_2$]; that is, heterodimers continuously exchange their EGF–EGFR segment with predimers and form homodimers [(EGF-EGFR)$_2$]. Also, the current work shows that lateral activation of EGFR and cell signal amplification take place through reversible association of heterodimers into homodimers.

## Results and Discussion

Uniform distribution of QD-labeled EGF-EGFR complexes were generated in the cell membrane by activating the cells with solutions of QD-EGF in phosphate buffered saline (PBS; 0.5 to 2 nM). Figure 1A shows the fluorescence image

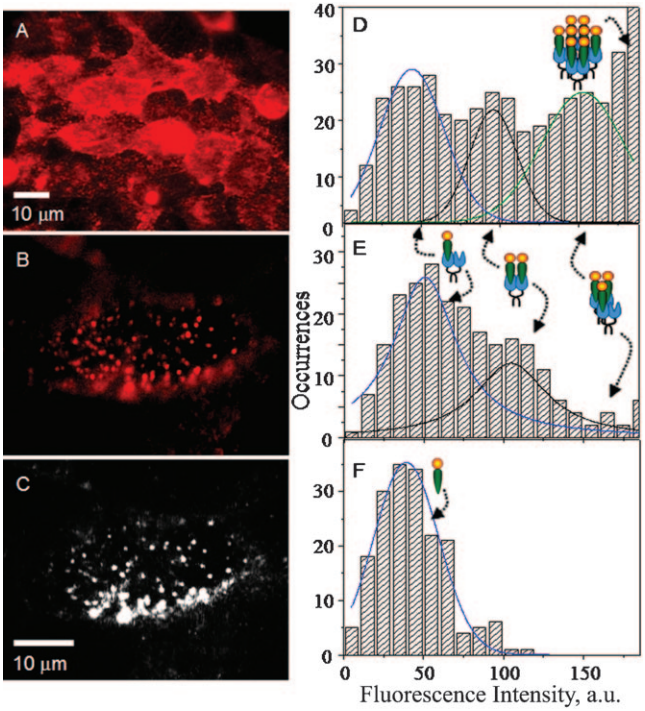


Figure 1. A) Florescence image of living A431 cells activated with 2 nM QD-EGF. B) Fluorescence and C) FRET images of an A431 cell labeled with Cy5-Ab11 and activated with 0.5 nM QD-EGF. D) and E) Histograms of fluorescence intensity from A431 cells activated with D) 2 nM and E) 0.5 nM QD-EGF. F) Histogram of fluorescence intensity from QD-EGF single molecules without cells. The solid curves in D) and E) are a guide for the eyes. The statistical distributions of heterodimers, homodimers and oligomers of EGFR were estimated from Gaussian fits.

of A431 cells 1 h after activation with a solution of QD-EGF in PBS (2 nM). Figure 1B and C shows the fluorescence and FRET images, respectively, of an A431 cell labeled with a solution Cy5-Ab11 in PBS (0.5 nM) followed by activation with a solution QD-EGF in PBS (0.5 nM). FRET signal was collected through a band-pass filter for Cy5 fluorescence. The bright fluorescence areas in Figure 1A were due to oligomers and clusters of QD-EGF-EGFR (movie 1 in the Supporting Information), while the isolated fluorescence spots in Figure 1B were due to EGFR single molecules (movie 2 in the Supporting Information). Figure 1D and E shows histograms of the fluorescence intensity spots in cells activated with solutions of QD-EGF in PBS at 2 and 0.5 nM, respectively. Figure 1F shows a histogram of the fluorescence intensity for QD-EGF single molecules in the cell culture medium, but without cells. Based on the fluorescence intensity, which is approximately 50 for QD-EGF (Figure 1F), it is apparent that the intensities, roughly 50,

  

100, 150, and ≥180 in Figure 1D and E, were due to one, two, three, and groups of QD-EGF-EGFR complexes. EGFRs mostly exist as dimers, oligomers, and clusters, whereas monomers of EGFR are unstable.[5–15] Thus, the intensities, roughly 50 and 100, in Figure 1D and E, were probably due to heterodimers [QD-EGF-$(EGFR)_2$] and homodimers [$(QD\text{-}EGF\text{-}EGFR)_2$] of EGFRs, respectively. Also, fluorescence intensity >150 was due to oligomers and clusters of EGFR. The distribution of heterodimers, homodimers, and clusters in cells activated with a solution of QD-EGF in PBS (2 nM) was 1:0.72:1.1 (Figure 1D). Note that fluorescence spots with intensities exceeding the saturation level (>185) of the CCD camera were not included in the histograms. The distribution of heterodimers and homodimers in cells activated with a solution of QD-EGF in PBS (0.5 nM) was 1:0.52 (Figure 1E). Thus, by activating EGFR with a solution of QD-EGF in PBS (0.5 nM), a large number of heterodimers were generated in the cell membrane.

Indications of long-range and reversible propagation of EGFR activation were obtained by single-molecule imaging (movies 2 and 3 in the Supporting Information). To investigate the speed and the reversibility of lateral propagation, we recorded and analyzed the fluorescence images and trajectories of single molecules. Figure 2A shows the fluorescence image of EGFR single molecules labeled by QD-EGF in an A431 cell. Figure 2B shows the typical propagation

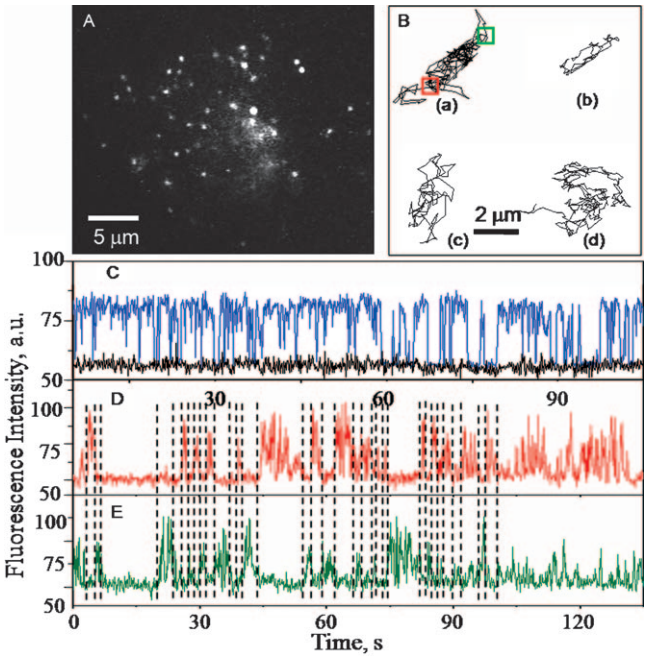


Figure 2. A) Fluorescence image of an A431 cell activated with 0.5 nM QD-EGF. B) Lateral propagation trajectories for four heterodimers in A. C)–E) Fluorescence intensity trajectories of single molecules: C) trajectory of an isolated stationary spot, D) trajectory of a propagating heterodimer recorded at the red window marked in B, and E) trajectory of the same heterodimer recorded at the green window marked in B. The increase and decrease in the intensities in C and D represent the exit time of the heterodimer at the green window and its subsequent entry time at the red window and vice versa. Vertical lines in D and E represent appearance and disappearance of single molecules in the two windows.

trajectories for four heterodimers. Each trajectory was obtained by tracing the threshold fluorescence intensity, equivalent to the intensity of a heterodimer, on 1000 to 5000 images at intervals of 33 ms. The mean square displacement ($MSD = \langle r(t)^2 \rangle$) during the activation was estimated from the distance ($r$) and time ($t$) between the steps.[65] Details of data acquisition and analysis are provided in the Supporting Information. Interestingly, around 30% of the propagating fluorescence spots followed near-linear back-and-forth trajectories (traces a and b in Figure 2B). Also, examples of random propagation trajectories are shown by traces c and d in Figure 2B. Both linear and random trajectories laterally extend up to 3 μm, indicating that the microdomain size for EGFR activation can be as large as 7 $\mu m^2$.[21,45–47] The linear trajectories indicate that the activation of EGFR propagated along predimers bound to the cytoskeleton. In other words, the linear trajectories support previous reports on the restricted propagation of EGFR resulting from predimers that are bound to the cytoskeleton.[19,25,45–48] To further characterize the speed and reversibility of EGFR activation, we recorded and analyzed both time- and distance-correlated single-molecule fluorescence intensity trajectories. Figure 2C shows the fluorescence intensity trajectory of a stationary heterodimer, which is equivalent to the "on/off" trajectory of a single QD.[52,55,56,61,66] Figure 2D and E shows the fluorescence intensity trajectories of a heterodimer recorded at two single-molecule windows (red and green squares) set 3 μm apart on trajectory a in Figure 2B. The trajectories were constructed in tandem by continuously collecting the fluorescence intensities in the two windows. The increase and decrease in the intensities in Figure 2D, correspondingly, indicate the time at which a heterodimer entered and left the red window. The increase and decrease in the intensities in Figure 2E, respectively, indicate the time at which a heterodimer subsequently entered and left the green window. Nevertheless, the fluctuations of fluorescence intensity were also contributed by blinking of quantum dots due to Auger ionization.[52,55,56,61,66] From the propagation path and the time stamping in the windows, we not only estimated the speed of EGFR activation, but also determined that EGFR activation reversibly propagated in the cell membrane. The statistical distribution of the activation speed for EGFR single molecules and the details for data acquisition and analysis are given in the Supporting Information. Here, we detected the long-range propagation of EGFR activation, owing to a combination of the exceptional photostability of QDs[52,53,58] and extended time- and distance-correlated single-molecule imaging (movie 2 in the Supporting Information) that was implemented. On the other hand, the photobleaching of organic dyes and fluorescent proteins in previous investigations probably prevented the detection and analysis of the long-range and reversible activation of EGFR.[15,19,25]

To investigate the mechanism underlying the reversible activation, we recorded and analyzed the fluorescence intensity trajectories of activated EGFR single molecules. Figure 3A shows the intensity trajectory of a stationary hetero-

  

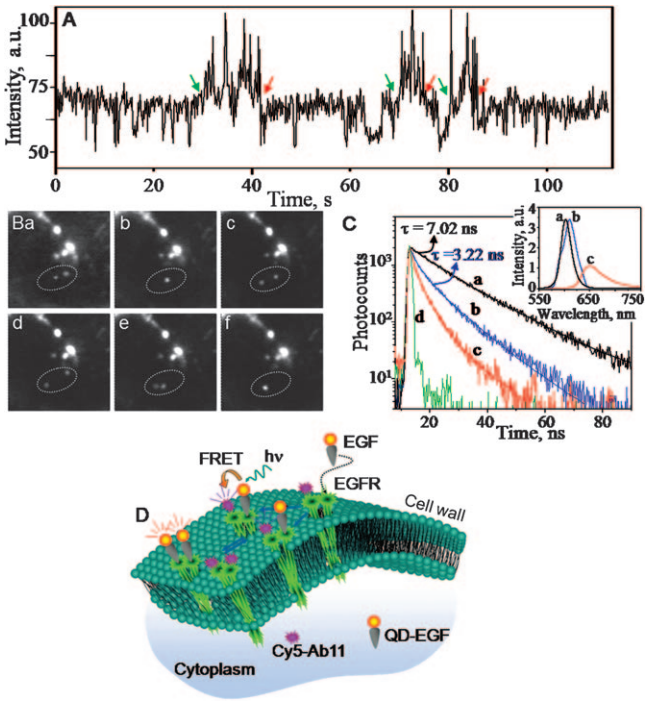


Figure 3. A) Single-molecule fluorescence intensity trajectory of a heterodimer. The arrows indicate the formation (green) and dissociation (red) of homodimers [(QD-EGF-EGFR)2]. B) FRET images of two heterodimers (marked area) in an A431 cell labeled with Cy5-Ab11 and activated with QD-EGF. C) Fluorescence decay profiles of QD and Cy5 in an A431 cell: a) decay of QD without Cy5-Ab11 labeling, b) decay of QD with Cy5-Ab11 labeling, c) decay of Cy5 at 670 nm as a result of FRET, and d) instrument response function. Inset, fluorescence spectra of a QD-EGF in a single cell: a) without Cy5-Ab11 labeling (no FRET) and b) with Cy5-Ab11 labeling (FRET from QD to Cy5). D) Schematic representation of the reversible propagation of EGFR activation on a cell membrane.

dimer in the proximity of a propagating heterodimer. Favorably, the propagating heterodimer reversibly associated with and dissociated from the stationary heterodimer, causing transient increases and decreases (green and red arrows in Figure 3A) in the fluorescence intensities. The increase in the intensity indicates that two heterodimers [QD-EGF-$(EGFR)_2$] have associated into a homodimer (QD-EGF-$EGFR)_2$ and a predimer $(EGFR)_2$, while the successive decrease in the intensity indicates that the homodimer has dissociated into two heterodimers (Scheme 1 in the Supporting Information). Thus, the repeated increase and decrease in the fluorescence intensity in Figure 3A indicate repeated formation and dissociation of signaling dimers. In other words, reversible association of heterodimers is the origin of multiple signaling or cell-signal amplification. Although the formation of homodimers, resulting from cooperative interactions between heterodimers and predimers, was reported,[15,19,25] to the best of our knowledge reversible association of heterodimers into homodimers remained obscured until the current work.

Because of the optical limitation, single-molecule imaging alone was insufficient to correlate the increase and decrease in fluorescence intensity with the reversible association and dissociation of EGFR. For example, an increase in the fluorescence intensity (Figure 3A) can be due to simple crossover between two heterodimers within the diffraction limited fluorescence image. Thus, we further investigated the activation of EGFR using FRET from QD-labeled EGF-EGFR to Cy5-labeled EGFR (Scheme 1 in the Supporting Information). The advantage of FRET over single-molecule fluorescence imaging is that the former is sensitive to nanometer-scale variations in the distance between a donor and an acceptor.[67–70] Figure 3B shows FRET images of activated EGFR molecules in a cell. The areas that are marked in Figure 3B show two propagating FRET spots. FRET itself suggested that QD-EGF-EGFR and Cy5-Ab11-EGFR were associated into heterodimers (QD-EGF-EGFR-EGFR-Ab11-Cy5). Thus, the propagation of FRET spots indicates that a heterodimer continuously exchanged its QD-EGF-EGFR segment with the Cy5-Ab11-EGFR segments in predimers. Yet another possibility that a heterodimer laterally diffused without dissociation was ruled out, because the FRET spots transiently associated and then disappeared. The association of two FRET spots indicates that the two heterodimers were in close proximity, and the disappearance of FRET indicates that the two heterodimers had transformed into two homodimers, $(QD\text{-}EGF\text{-}EGFR)_2$ and $(Cy5\text{-}Ab11\text{-}EGFR)_2$, through an exchange of their monomers. As stated above, disappearance of the fluorescence/FRET spots was also contributed by blinking. Additional data indicating the association and disappearance of FRET spots are given in the Supporting Information. FRET from QD-EGF-EGFR to Cy5-Ab11-EGFR and the exchange of monomers between two heterodimers, and the formation of homodimers are schematically shown in Figure 3D. The disappearance of FRET is understandable as the homodimers, which lack both donors and acceptors in the same dimer, do not show FRET. Thus, the single-molecule fluorescence intensity trajectory (Figure 3A) and the FRET images (Figure 3B) support the notion that the lateral propagation of EGFR activation takes place reversibly by an exchange of monomers between activated EGFR and predimers.

To investigate FRET in cells that were activated with QD-EGF and labeled with Cy5- Ab11, fluorescence decays (Figure 3C) and time-resolved fluorescence spectra (inset of Figure 3C) were recorded and analyzed. Figure 3C shows the fluorescence decay profiles of activated single-cells with (trace b) and without (trace a) Cy5-Ab11 labeling. We found that the average lifetime of QDs decreased from $\tau_{av} = 7.02 \pm 0.25$ ns for cells without Cy5-labeling to $\tau_{av} = 3.22 \pm 0.12$ ns for cells labeled with Cy5. The average lifetime values were obtained by fitting multi-exponential decays (traces a and b in Figure 3C) to the third-order kinetic equation. Also, the decrease in the lifetime of QDs was associated with fluorescence emission from Cy5 (trace c in Figure 3C and trace b in the inset of Figure 3C). The decrease in the fluorescence lifetime of energy donor (QD) and the concomitant fluorescence from energy acceptor (Cy5) verify the FRET activity from QD-EGF-EGFR to Cy5-Ab11-EGFR. In other words,

  

decrease in the fluorescence lifetime of QDs indicate that the lateral propagation of EGFR activation takes place through continuous exchange of monomers among heterodimers and predimers.

To further investigate the interactions between heterodimers with predimers, we correlated single-molecule fluorescence images with the topography of activated cells. Figure 4 shows correlated optical and AFM images of an

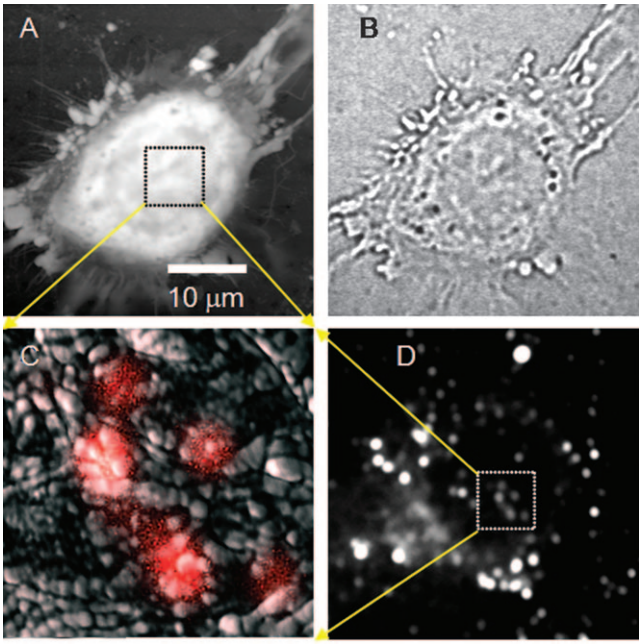


Figure 4. Correlated optical/AFM images of an A431 cell activated with QD-EGF. A) AFM image, B) optical transmission image, C) correlated fluorescence/AFM image of a zoomed-in and scanned portion in A, and D) fluorescence image. The red spots in C) show fluorescence from activated EGFR.

A431 cell activated with a solution QD-EGF in PBS (0.5 nM). Figure 4C shows a zoomed-in and scanned AFM image of the cell correlated with the fluorescence spots in Figure 4D. The AFM image indicated the presence of a large number of nanostructures on the cell membrane, which should come from various membrane proteins, glycolipids, and so on. In other words, because of the non-specific nature of imaging, AFM alone was insufficient to pinpoint an activated EGFR single molecule on the cell surface. On the other hand, because of the specific binding between EGF and EGFR, the fluorescence spots in Figure 4C and D were due to QD-EGF-EGFR complexes. The topography of the correlated image indicated that the activated EGFR molecules were associated with clusters composed of a large number of identical structures. In addition, it has been reported that EGFR molecules form oligomers and clusters on the cell membrane.[6–14,18–29,45–47] Thus, we assumed that the clusters in the topography image, overlaid by the fluorescence spots (Figure 4C), were due to activated EGFR molecules that coexisted with predimers. Indeed, the dynamic nature of cell surface structures and slow scanning in AFM imaging prevented us from obtaining real-time and reproducible AFM images of activated EGFR single molecules. Although EGFR dimers were not detected as isolated structures (Supporting Information), the coexistence of activated EGFR with predimers is consistent with both previous reports on the existence of EGFR as oligomers and the current single-molecule fluorescence and FRET results regarding the transient dimerization of an activated EGFR.

## Conclusion

We have investigated the extent and the mode of EGFR activation in living cells using single-molecule fluorescence imaging and FRET. Owing to the exceptional photostability of QDs, we determined that reversible association of heterodimers into homodimers stimulates multiple signaling, and the lateral propagation of EGFR activation takes place through the transient dimerization of a heterodimer with predimers. How an activated EGFR laterally activates a large number of predimers is relevant not only to our understanding of the EGFR pathway in cell-signaling, but also for designing EGFR-targeted therapeutic molecules in an effort to control cancers.

## Experimental Section

**Materials**. Recombinant human EGF, 3-sulfo-*N*-hydroxysuccinimide ester, mouse monoclonal EGFR antibody (Ab11), heat-inactivated fetal bovine serum (FBS), phosphate buffered saline (PBS), tripsin solution and sephadex-G25 resin column were obtained from Sigma. QD-strepatavidin conjugate and Cy5-streptavidin conjugate were obtained from Invitrogen Corporation and Biocompare, respectively. Dulbecco's modified Eagle's medium (DMEM) was obtained from Gibco. The samples and reagents were used as obtained without further purification.

**Labeling EGF ligand and Ab11 suing QDs and Cy5**. We labeled EGF and Ab11 with streptavidin conjugated CdSe-ZnS QDs or streptavidin conjugated Cy5 through biotin-avidin linkage. Recombinant human EGF was reconstituted in PBS at 200 $\mu g\,mL^{-1}$ and biotinylated using 3-sulfo-*N*-hydroxysuccinimide ester at room temperature. The biotinylated EGF was purified by gel filtration on sephadex-G25 resin. The concentration of the purified EGF-biotin conjugate was set to 50 nM with PBS, and this conjugate was reacted with a solution (50 nM in PBS) of QD–streptavidin conjugate at room temperature for 30 min. These steps were repeated for labeling Ab11. EGF was labeled with deep-red fluorescent QDs ($\lambda_{max} \approx 650$ nm) for colocalization experiments and red fluorescent QDs (λmax ~605 nm) for single-molecule imaging and FRET experiments. The antibody was labeled with green fluorescent QDs ($\lambda_{max} \approx 560$ nm) for colocalization experiments and Cy5-streptavidin for FRET experiments.

**Cell culture and labeling.** A431 cells were cultured up to ≈60% confluence in DMEM medium containing 10% heat-inactivated FBS. The cells were washed five times with PBS and activated with QD-EGF conjugate (2 or 0.5 nM) for 1 h at 4°C. Following activation, the cells were washed five times with PBS and maintained in DMEM without FBS and phenol red. For colocalization of QD650-EGF and QD560-Ab11 conjugates, the cells were treated with QD560-Ab11 conjugate (0.5 nM) for 1 h at room temperature followed by QD650-EGF (0.5 nM) for 1 h at 4°C. Similarly, cell samples for single-molecule fluorescence imaging were prepared by treating the cells with QD605-EGF conjugates, and cell samples for

  

FRET experiments were prepared by treating the cells with Cy5-Ab11 conjugate.

**Single-molecule imaging, AFM imaging, and spectroscopy.** Fluorescence images of cells were obtained in an inverted optical microscope (Olympus IX70) equipped with an objective lens (Olympus PUlanApo 60X), band-pass filters for QDs and Cy5, an image intensifier (Hamamatsu-C8600) and a CCD camera (Hamamatsu-C5985 or Olympus). The fluorescence from cells was acquired as movie files (Supporting videos 1–3). Fluorescence and FRET images and propagation and intensity trajectories of single molecules were obtained by analyzing the videos using the AquaCosmos software program (Hamamatsu). Correlated optical/AFM images were obtained using an apparatus assembled from an inverted optical microscope (Olympus IX70) and an MFP-3D AFM (Asylum Research). The AFM was equipped with an ultra-sharp (radius of curvature $\approx$7 nm) silicon nitride cantilever (Olympus). A 488 nm continuous wave laser (Coherent-Sapphire 488–25 CDRH) was used as the excitation source for fluorescence imaging. Fluorescence decays and time-resolved fluorescence spectra were recorded using an apparatus assembled from a polychromator (Chromex-250IS) and a photon-counting streak-scope (Hamamatsu-C4334). Fluorescence lifetimes were obtained by fitting the decays to third order kinetics. For decay measurements, the excitation source consisted of 400 nm pulses (150 fs) generated from the second harmonic generation (SHG) crystal of an optical parametric amplifier (Coherent OPA 9400). The OPA was pumped at 200 kHz by a regenerative amplifier (Coherent RegA 9000) that was seeded by a mode-locked Ti:Sapphire laser (Coherent Mira 900F).

## Acknowledgements

V.B. and M.I. gratefully acknowledge support from Japan Science and Technology Agency.

[1] B. S. Khakh, R. A. North, *Nature* **2006**, *442*, 527–532.
[2] C. H. Heldin, *Cell* **1995**, *80*, 213–223.
[3] D. M. Anderson, E. Maraskovsky, W. L. Billingsley, W. C. Dougall, M. E. Tometsko, E. R. Roux, M. C. Teepe, R. F. DuBose, D. Cosman, L. Galibert, *Nature* **1997**, *390*, 175–179.
[4] Y. G. Shi, J. Massague, *Cell* **2003**, *113*, 685–700.
[5] S. Wullschleger, R. Loewith, M. N. Hall, *Cell* **2006**, *124*, 471–484.
[6] P. Yaish, A. Gazit, C. Gilon, A. Levitzki, *Science* **1988**, *242*, 933–935.
[7] J. Schlessinger, *Cell* **2000**, *103*, 211–225.
[8] R. Jorissen, N. F. Walker, N. Pouliot, T. P. J. Garrett, C. W. Ward, A. W. Burgess, *Exp. Cell Res.* **2003**, *284*, 31–53.
[9] G. Carpenter, S. Cohen, *J. Biol. Chem.* **1990**, *265*, 7709–7712.
[10] J. Schlessinger, *Cell* **2002**, *110*, 669–672.
[11] Y. Yarden, J. Schlessinger, *Biochemistry* **1987**, *26*, 1434–1442.
[12] P. Klein, D. Mattoon, M. A. Lemmon, J. Schlessinger, *Proc. Natl. Acad. Sci. USA* **2004**, *101*, 929–934.
[13] Y. Yarden, A. Ullrich, *Annu. Rev. Biochem.* **1988**, *57*, 443–478.
[14] T. W. J. Gadella, T. M. Jovin, *J. Cell Biol.* **1995**, *129*, 1543–1558.
[15] Y. Teramura, J. Ichinose, H. Takagi, H. Nishida, T. Yanagida, Y. Sako, *Embo J.* **2006**, *25*, 4215–4222.
[16] G. T. Merlino, Y. H. Xu, S. Ishii, A. L. J. Clark, K. Semba, K. Toyoshima, T. Yamamoto, I. Pastan, *Science* **1984**, *224*, 417–419.
[17] J. Mendelsohn, J. Baselga, *Oncogene* **2000**, *19*, 6550–6565.
[18] J. Ichinose, M. Murata, T. Yanagida, Y. Sako, *Biochem. Biophys. Res. Commun.* **2004**, *324*, 1143–1149.
[19] A. R. Reynolds, C. Tischer, P. J. Verveer, O. Rocks, P. I. H. Bastiaens, *Nat. Cell Biol.* **2003**, *5*, 447–453.
[20] M. Offterdinger, V. Georget, A. Girod, P. I. H. Bastiaens, *J. Biol. Chem.* **2004**, *279*, 36972–36981.
[21] Z. Xiao, X. Ma, Y. Jiang, Z. Zhao, B. Lai, J. Liao, Y. Yue, X. Fang, *J. Phys. Chem. B* **2008**, *112*, 4140–4145.
[22] M. A. Lemmon, Z. Bu, J. E. Ladbury, M. Zhou, D. Pinchasi, I. Lax, D. Engelman, J. Schlessinger, *Embo J.* **1997**, *16*, 281–294.
[23] Y. Yarden, M. X. Sliwkowski, *Nat. Rev. Mol. Cell Biol.* **2001**, *2*, 127–137.
[24] T. Uyemura, H. Takagi, T. Yanagida, Y. Sako, *Biophys. J.* **2005**, *88*, 3720–3730.
[25] Y. Sako, S. Minoghchi, T. Yanagida, *Nat. Cell Biol.* **2000**, *2*, 168–172.
[26] C. X. Yu, J. Hale, K. Ritchie, K. N. Prasad, J. Irudayaraj, *Biochem. Biophys. Res. Commun.* **2009**, *378*, 376–382.
[27] S. E. D. Webb, S. K. Roberts, S. R. Needham, C. J. Tynan, D. J. Rolfe, M. D. Winn, D. T. Clarke, R. Barraclough, M. L. Martin-Fernandez, *Biophys. J.* **2008**, *94*, 803–819.
[28] S. Saffarian, Y. Li, E. L. Elson, L. J. Pike, *Biophys. J.* **2007**, *93*, 1021–1031.
[29] M. Morimatsu, H. Takagi, K. G. Ota, R. Iwamoto, T. Yanagida, Y. Sako, *Proc. Natl. Acad. Sci. USA* **2007**, *104*, 18013–18018.
[30] W. E. Moerner, *J. Phys. Chem. B* **2002**, *106*, 910–927.
[31] J. Hofkens, M. Maus, T. Gensch, T. Vosch, M. Cotlet, F. Kohn, A. Herrmann, K. Mullen, F. de Schryver, *J. Am. Chem. Soc.* **2000**, *122*, 9278–9288.
[32] V. Biju, M. Micic, D. Hu, H. P. Lu, *J. Am. Chem. Soc.* **2004**, *126*, 9374–9381.
[33] P. Tinnefeld, M. Sauer, *Angew. Chem.* **2004**, *117*, 2698–2628; *Angew. Chem. Int. Ed.* **2004**, *43*, 2642–2671.
[34] W. E. Moerner, M. Orrit, *Science* **1999**, *283*, 1670–1676.
[35] S. Weiss, *Science* **1999**, *283*, 1676–1683.
[36] D. M. Kong, Y. E. Ma, J. Wu, H. X. Shen, *Chem. Eur. J.* **2009**, *15*, 901–909.
[37] E. Braeken, G. de Cremer, P. Marsal, G. Pepe, K. Mullen, R. A. L. Vallee, *J. Am. Chem. Soc.* **2009**, *131*, 12201–12210.
[38] S. Rocha, J. A. Hutchison, K. Peneva, A. Herrmann, K. Muellen, M. Skjot, C. I. Jorgensen, A. Svendsen, F. C. De Schryver, J. Hofkens, H. Uji-i, *ChemPhysChem* **2009**, *10*, 151–161.
[39] T. Lebold, L. A. Muhlstein, J. Blechinger, M. Riederer, H. Amenitsch, R. Kohn, K. Peneva, K. Mullen, J. Michaelis, C. Brauchle, T. Bein, *Chem. Eur. J.* **2009**, *15*, 1661–1672.
[40] A. Katranidis, D. Atta, R. Schlesinger, K. H. Nierhaus, T. Choli-Papadopoulou, I. Gregor, M. Gerrits, G. Buldt, J. Fitter, *Angew. Chem.* **2009**, *121*, 1790–1793; *Angew. Chem. Int. Ed.* **2009**, *48*, 1758–1761.
[41] D. Wöll, E. Braeken, A. Deres, F. C. De Schryver, H. Uji-i, J. Hofkens, *Chem. Soc. Rev.* **2009**, *38*, 313–328.
[42] F. Hillger, D. Haenni, D. Nettels, S. Geister, M. Grandin, M. Textor, B. Schuler, *Angew. Chem.* **2008**, *120*, 6279–6283; *Angew. Chem. Int. Ed.* **2008**, *47*, 6184–6188.
[43] D. Nishimura, Dai, Y. Takashima, H. Aoki, T. Takahashi, H. Yamaguchi, S. Ito, A. Harada, *Angew. Chem.* **2008**, *120*, 6166–6168; *Angew. Chem. Int. Ed.* **2008**, *47*, 6077–6079.
[44] A. Y. Kobitski, M. Hengesbach, M. Helm, G. U. Nienhaus, *Angew. Chem.* **2008**, *120*, 4398–4402; *Angew. Chem. Int. Ed.* **2008**, *47*, 4326–4330.
[45] G. Orr, D. Hu, S. Ozcelik, L. K. Opresko, H. S. Wiley, S. D. Colson, *Biophys. J.* **2005**, *89*, 1362–1373.
[46] J. C. den Hartigh, P. M. van Bergen en Henegouwen, A. J. Verkleij, J. Boonstra, *J. Cell Biol.* **1992**, *119*, 349–355.
[47] D. Tang, D. J. Gross, *Biochem. Biophys. Res. Commun.* **2003**, *312*, 930–936.
[48] Y. Sako, A. Nagafuchi, S. Tsukita, M. Takeichi, A. Kasumi, *J. Cell Biol.* **1998**, *140*, 1227–1240.
[49] C. B. Murray, D. J. Norris, M. G. Bawendi, *J. Am. Chem. Soc.* **1993**, *115*, 8706–8715.
[50] W. C. W. Chan, S. Nie, *Science* **1998**, *281*, 2016–2018.
[51] M. P. Bruchez, Jr., M. Moronne, P. Gin, S. Weiss, A. P. Alivisatos, *Science* **1998**, *281*, 2013—2016.
[52] V. Biju, T. Itoh, A. Anas, A. Sujith, M. Ishikawa, *Anal. Bioanal. Chem.* **2008**, *391*, 2469—2495.
[53] X. Y. Wu, H. J. Liu, J. Q. Liu, K. N. Haley, J. A. Treadway, J. P. Larson, N. F. Ge, F. Peale, M. P. Bruchez, *Nat. Biotechnol.* **2003**, *21*, 41–46.

  

[54] V. Biju, Y. Makita, A. Sonoda, H. Yokoyama, Y. Baba, M. Ishikawa, *J. Phys. Chem. B* **2005**, *109*, 13899–13905.
[55] J. Tang, R. A. Marcus, *Phys. Rev. Lett.* **2005**, *95*, 107401.
[56] V. Biju, Y. Makita, T. Nagase, Y. Yamaoka, H. Yokoyama, Y. Baba, M. Ishikawa, *J. Phys. Chem. B* **2005**, *109*, 14350–14355.
[57] V. Biju, T. Itoh, Y. Baba, M. Ishikawa, *J. Phys. Chem. B* **2006**, *110*, 26068–26074.
[58] V. Biju, R. Kanemoto, Y. Matsumoto, S. Ishii, S. Nakanishi, T. Itoh, Y. Baba, M. Ishikawa, *J. Phys. Chem. C* **2007**, *111*, 7924–7932.
[59] V. Biju, D. Muraleedharan, K. Nakayama, Y. Shinohara, T. Itoh, Y. Baba, M. Ishikawa, *Langmuir* **2007**, *23*, 10254–10261.
[60] I. L. Medintz, H. T. Uyeda, E. R. Goldman, H. Mattoussi, *Nat. Mater.* **2005**, *4*, 435–446.
[61] Y. Matsumoto, R. Kanemoto, T. Itoh, S. Nakanishi, M. Ishikawa, V. Biju, *J. Phys. Chem. C* **2008**, *112*, 1345–1350.
[62] R. Kanemoto, A. Anas, Y. Matsumoto, R. Ueji, T. Itoh, Y. Baba, S. Nakanishi, M. Ishikawa, V. Biju, *J. Phys. Chem. C* **2008**, *112*, 8184–8191.
[63] A. Anas, H. Akita, H. Harashima, T. Itoh, M. Ishikawa, V. Biju, *J. Phys. Chem. B* **2008**, *112*, 10005–10011.
[64] A. Anas, T. Okuda, N. Kawashima, K. Nakayama, T. Itoh, M. Ishikawa, V. Biju, *ACS NANO* **2009**, *3*, 2419–2429.
[65] A. Kusumi, Y. Sako, M. Yamamoto, *Biophys. J.* **1993**, *65*, 2021–2040.
[66] M. Nirmal, B. O. Dabbousi, M. G. Bawendi, J. J. Macklin, J. K. Trautman, T. D. Harris, L. E. Brus, *Nature* **1996**, *383*, 802–804.
[67] J. R. Lakowicz, *Principles of Fluorescence Spectroscopy*, 2nd ed., Kluwer Academic, New York **1990**.
[68] T. Ha, *Methods* **2001**, *25*, 78–86.
[69] I. L. Medintz, A. R. Clapp, H. Mattoussi, E. R. Goldman, B. Fisher, J. M. Mauro, *Nat. Mater.* **2005**, *4*, 630–638.
[70] B. Schuler, *ChemPhysChem* **2005**, *6*, 1206–1220.

Received: October 27, 2009
Published online: December 18, 2009

  